ACS Macro Letters

Letter

pubs.acs.org/macroletters

Fracture-Healing Kinetics of Thermoreversible Physical Gels Quantified by Shear Rheophysical Experiments

Travis L. Thornell,[†] Benjamin A. Helfrecht,[†] Scott A. Mullen,[‡] Abhishek Bawiskar,[†,§] and Kendra A. Erk*[,†]

[†]School of Materials Engineering and [‡]College of Science, Purdue University, West Lafayette, Indiana 47907, United States

Supporting Information

ABSTRACT: The fracture-healing behavior of model physically associating triblock copolymer gels was investigated with experiments coupling shear rheometry and particle tracking flow visualization. Fractured gels were allowed to rest for specific time durations, and the extent of strength recovered during the resting time was quantified as a function of temperature (20−28 °C) and gel concentration (5−6 vol %). Measured times for full strength recovery were an order of magnitude greater than characteristic relaxation times of the system. The Arrhenius activation energy for post-fracture strength recovery was found to be greater than the activation energy associated with stress relaxation, most likely due to the entropic barrier related to the healing mechanism of dangling chain reassociation with network junctions.

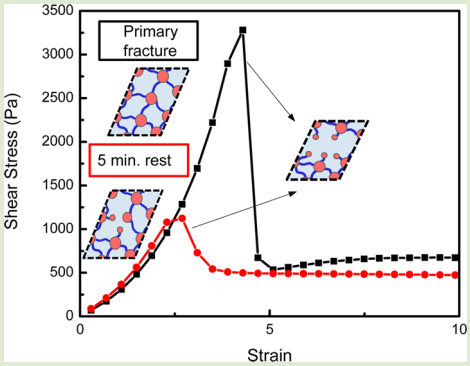

Soft materials with well-defined mechanical properties are important in a variety of industrial and biomedical applications, including high toughness elastomers for seals and dampers,[1] hydrogels for synthetic cartilage,[2] hemostatic materials for wound dressing,[3] injectable materials for regenerative medicine,[4,5] and superabsorbent polymer hydrogels for applications as diverse as drug delivery to cement internal curing agents.[6] To exhibit optimum performance in these applications, the material's mechanical response to large applied deformations and their ability to heal following damage must be well understood. However, these nonlinear mechanical properties are difficult to characterize for soft materials using traditional experimental techniques. Standard tension and compression mechanical tests require self-supported samples and are thus not appropriate for materials that have fast relaxation times or contain large amounts of solvent.

Recent work has shown shear rheometry to be an effective technique for characterizing the nonlinear deformation and fracture of soft materials.[7−10] To correlate the measured rheological response with the sample's macroscale behavior (e.g., formation of a fracture plane), rheophysical experiments are performed to simultaneously measure the local velocity profile during shear by employing a variety of techniques, including optical particle tracking,[11] ultrasonic velocimetry,[12] and NMR.[13]

In this letter, we describe a rheophysical methodology for quantifying the fracture and self-healing behavior of a soft material. A temperature-dependent, physically associating polymer gel will be utilized as a model soft material. Shear rheometry coupled with an optical particle tracking system was used to directly observe the shear-induced formation and subsequent healing of the fracture plane within the material. Compared to the characteristic stress relaxation behavior, fracture-healing occurred over much greater time scales but with similar temperature dependence. Activation energy for healing was found to be greater than for relaxation, most likely due to the entropic barrier required for a chain to reassociate with a network junction.

The model soft material is composed of triblock copolymer molecules dissolved in a midblock-selective solvent. The copolymer contains 8900 g/mol poly(methyl methacrylate) (PMMA) end blocks separated by a 53000 g/mol poly(*n*-butyl acrylate) (PnBA) midblock. At temperature (T) < 34 °C, the copolymer self-assembles into a three-dimensional network of flexible midblock segments, or "bridges", interconnected by spherical end block aggregates (details described elsewhere[14]). Previous studies have investigated the mechanical behavior of this material up to the point of failure[7,8,11,14] but have not yet addressed the postfracture healing response.

Gels are loaded into Couette rheometer cell above their critical temperature of 34 °C and cooled at a rate of 2 °C/min to the specified testing temperature (20−28 °C). The gels are then sheared at a constant shear rate ($\dot{\gamma}$) of 1 s^{-1} to measure the stress response resulting from shear-induced failure, referred to here as "primary fracture". The fractured gel is allowed to sit undisturbed at specific resting times (5 min to 14 h) and is then deformed at the same shear rate to obtain the "recovery fracture" stress response. The extent of strength recovery in the gel was determined from the ratio of the maximum shear stress for the recovery and primary fracture events. All fracture events were confirmed by measuring the local velocity of the gel across the width of the rheometer cell gap (1.5 mm) utilizing a

Received: August 25, 2014
Accepted: October 1, 2014
Published: October 6, 2014

 © 2014 American Chemical Society dx.doi.org/10.1021/mz500524d | *ACS Macro Lett.* 2014, 3, 1069−1073

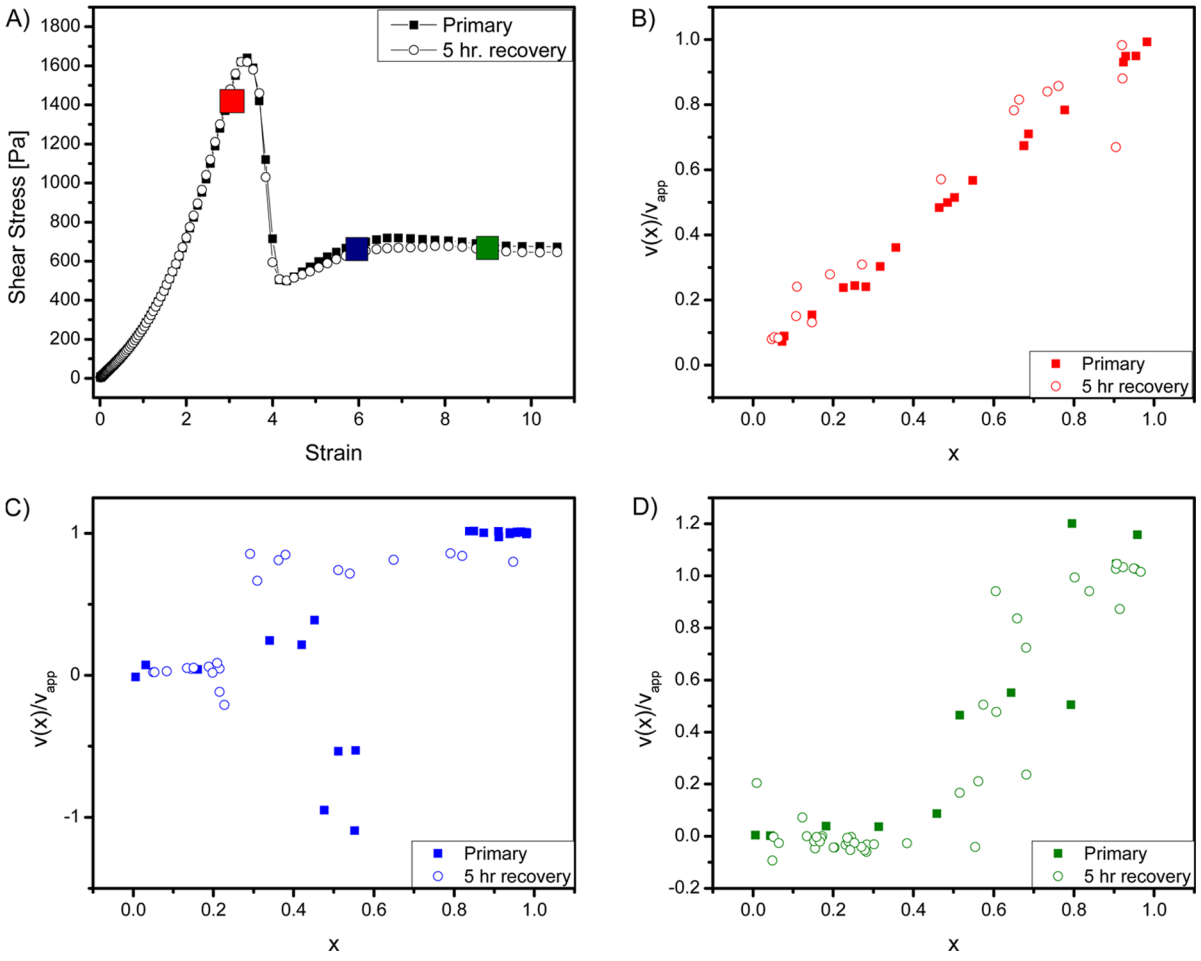

Figure 1. (A) Primary and 5 h recovery of a 5.5 vol % gel at 25 °C. Velocity profiles for three different strains during the primary and recovery events: (B) 3, (C) 6, and (D) 9 strain units. For B–D, the vertical axes reports the local velocity, $v(x)$, normalized by the applied velocity, v_{app} (1.41 mm/s), and the horizontal axes reports the location, x, within the normalized gap width (gap = 1.5 mm), where $x = 0$ is the location of the stationary wall of the rheometer and $x = 1$ is the location of the moving wall. For (D), $v(x)$ greater than 1 resulted from the motion of fracture-induced voids within the sample.

custom-built particle tracking flow visualization system coupled to the rheometer. To achieve this, the gel (which is transparent) was seeded with ppm concentration of inert particles. More details about these experiments are described in Supporting Information.

Figure 1 indicates the stress responses and corresponding velocity profiles of the primary and recovery fracture events. Focusing first on the primary fracture response (closed symbols in Figure 1), the gel's behavior can be investigated as a function of strain. A linear velocity profile was observed in Figure 1b that indicated a uniform elastic response of the network at a strain of 3. Prior work has shown that the observed stress response maximum and sharp decrease is a direct results of the shear-induced strain localization in the form of cohesive fracture of the gel.[11] The stress reduction is due to pull-out of elastically active chains within the polymer network[15,16] and formation of a region of dangling chains.[11] This fracture event was verified here: after the stress maximum, midgap fracture and elastic recoil are directly observed from the flow visualization data at a strain of 6, as seen in Figure 1c. The primary fracture plane appears to exist at $x = 0.6$, separating the section of the gel that is attached to the moving wall which maintains a fast positive velocity from the section of the gel attached to the stationary wall that transitions from near-zero relative velocity to displaying clear elastic recoil at the fracture plane (i.e., $v(x) < 0$). Figure 1d displays the postfracture velocity profile of the gel at a strain of 9.

The rheophysical results presented in Figure 1 are an example of the gel's ability to fully recover its strength during the 5 h resting time between the primary and recovery fracture events. After 5 h, the gel was able to reform the elastically active midblock bridges that allow for the recovered stress maximum response. The calculated velocity profiles for this recovery fracture showed similar characteristics. Most notably observed was a change in the fracture plane as seen in Figure 1c; the fracture site within the observation window shifted to about $x = 0.3$.

For shorter resting times, the extent of network recovery was a strong function of time. Figure 2a presents the stress–strain curves for primary fracture and subsequent recovery fracture events after resting times of 5–45 min for a 25 °C 5.5 vol % gel. At a rest time of 5 min, the percent recovery is at 45%. Increasing the rest time to 10, 30, and 45 min, the percent recovery increased to 59, 67, and 79%, respectively. The fracture plane of a partially recovered gel occurred at the same location as the primary fracture plane, as incomplete healing resulted in visible voids within the gel which acted as stress

dx.doi.org/10.1021/mz500524d | ACS Macro Lett. 2014, 3, 1069–1073

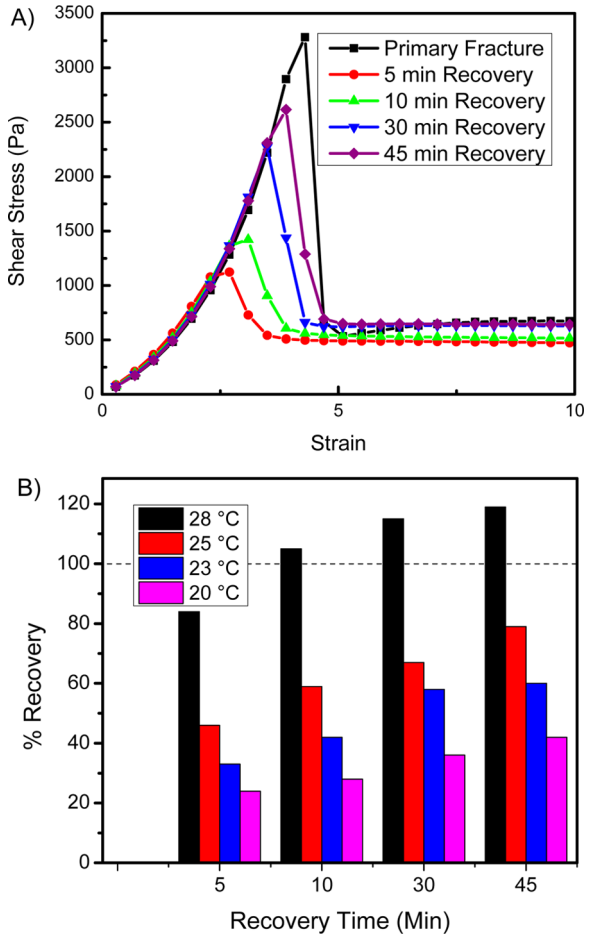

Figure 2. (A) Stress−strain curves of 25 °C 5.5 vol % gel with primary and resting times of 5−45 min; (B) percent recovery vs resting times of 5−45 min for temperatures ranging from 28 to 20 °C for a 5.5 vol % gel.

concentration sites and subsequently decreased the observed maximum stress response.

Given sufficient resting time, the network can regain its original strength, and the primary and recovery stress responses almost perfectly overlap (see Figure 1a). Strength recovery was found to be accelerated by increasing the temperature of the system. This is shown in Figure 2b. Gels at the higher temperatures of 28 and 25 °C were able to recover at a faster rate than gels at the lower temperatures of 23 and 20 °C.

The time for 100% strength recovery, referred to here as the "full recovery time", was determined from a power law fit to the experimental data (see Figure 3). Compared to direct experimental observation of full recovery, this was a preferred method to determine the full recovery time because at these much longer time scales (>250 min), solvent evaporation may begin to influence the data.

Degree of recovery was also found to be a strong function of gel concentration. Table 1 summarizes the full recovery times of 5, 5.5, and 6 vol % gels. For 5 vol % gels, the recovery times ranged from 3 to 670 min. As concentration is increased, the time ranges grow to 11−1100 min for 5.5 vol % and 25−1600 min for 6 vol %.

Arrhenius-type relationships of ln(1/recovery time) and inverse temperatures of 20−28 °C, as shown in Figure 4, allowed for the calculation of activation energies related to the recovery or "healing" behavior ($E_{a,rec}$). Recovery activation

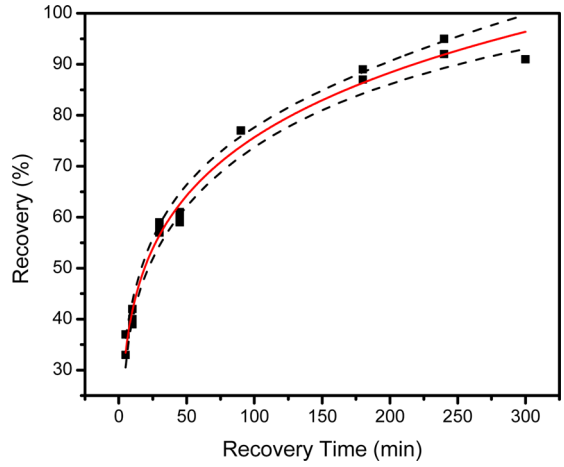

Figure 3. Recovery response of 23 °C, 5.5 vol % gel with 95% confidence intervals, described by $y = a + bx^n$, where y is percent recovery, x is recovery time; $a = -45$, $b = 62$, and $n = 0.14$ are fitting parameters.

Table 1. Full Recovery Times and Relaxation Times at Various Temperatures and Concentrations

concentration (vol %)	temperature (°C)	full recovery time (min)	relaxation time (sec)
5.0	28	3	2.4
	25	40	10
	23	150	50
	20	670	120
5.5	28	11	2.5
	25	50	20
	23	360	40
	20	1100	130
6.0	28	25	3
	25	210	20
	23	400	30
	20	1600	120

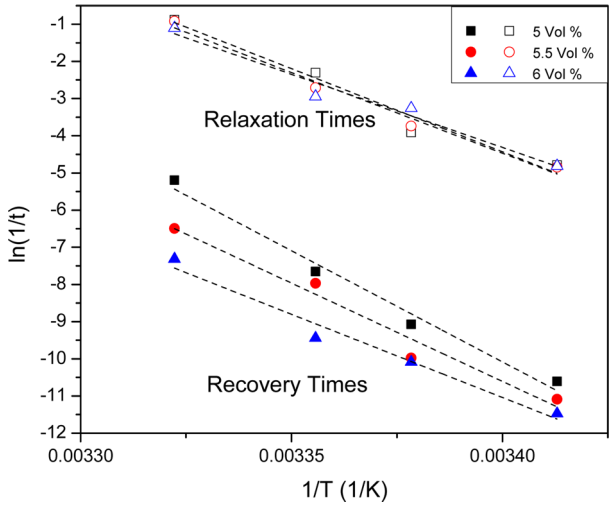

Figure 4. Arrhenius relationships where t (s) represents recovery times or characteristic relaxation times for the various gel concentrations.

energies were observed to decrease with increasing concentration: $E_{a,rec}$ = 500 kJ/mol for 5 vol % gel; 440 kJ/mol for 5.5 vol %; 370 kJ/mol for 6 vol %.

dx.doi.org/10.1021/mz500524d | ACS Macro Lett. 2014, 3, 1069−1073

Interestingly, previously reported characteristic stress relaxation times (τ) for these gels displayed a similar Arrhenius dependence on temperature.[8] Following previous methods, characteristic relaxation times for each gel concentration and temperature were determined from stretched exponential curve fits to step-strain experimental data (described in Supporting Information), in which a strain of 5% is applied to the gel and stress relaxation is measured as a function of time. These values of τ are reported in Table 1 and included in Figure 4, allowing for direct comparison with the observed recovery behavior.

From this data, activation energies related to the relaxation behavior ($E_{a,relax}$) were found to weakly dependent on gel concentration, with $E_{a,relax}$ = 370, 360, and 330 kJ/mol for 5, 5.5, and 6 vol % gels, respectively. In past work with higher concentration gels,[14] the activation energies determined from the Arrhenius dependence of relaxation times were believed to be related to the energy required for chain pull-out of a stressed, elastically active bridge from its network junction (i.e., end block aggregate).

One striking observation was that the relaxation times (sec to min) were over an order of magnitude smaller than the recovery times (min to hrs). This is most likely because the small strain nature of the step-strain experiments that probe the relaxation behavior do not deform the network as severely as the nonlinear, large strain fracture experiments which often resulted in macroscopic voids within the gel sample. For stress relaxation, the region of disorder caused by chain pull-out is on the order of tens of nm but is increased to on the order of μm-mm for shear-induced fracture. The initial gelation kinetics are a closer match to the time scales of recovery as both are comparable at the magnitude of minutes (included in Supporting Information).

The relaxation and recovery behaviors display similar dependences on temperature, with increasing temperature resulting in faster relaxation or recovery behavior of the gel. This is consistent with the thermoreversible nature of the physically associating triblock copolymer network and specifically the enthalpically driven self-assembly process to form the network. Both the relaxation and recovery behaviors also display similar dependence on gel concentration, with higher concentration gels having reduced activation energies.

For all gel systems investigated here, we observed that $E_{a,rec}$ was larger than $E_{a,relax}$. This implies that the energy required to insert a dangling end block into a network junction is greater than the energy required to remove an elastically active end block. Considering the thermodynamics of the system, there is an inherent entropic barrier for healing to occur, as healing requires a freely dangling chain to insert into an end block aggregate (or form a new aggregate). By comparison, it is entropically favorable to remove a chain from confinement within an aggregate. To better understand this behavior, including the enthalpic contribution to the behaviors, future studies will need to investigate the dependence of activation energy on end block molecular weight and solvent quality. Additionally, recent simulation results suggest that the relative aggregate size may change as a result of strong shear deformation and the shear-induced fracture and healing process.[17]

The gels were able to surpass their original strengths (>100% recovery) at 28 °C for all tested concentrations (see Figure 2b). The self-healing and eventual strengthening of gels at 28 °C cannot be attributed to a singular cause. The network structure at this relatively high temperature does exhibit solid-like gel characteristics but very fast relaxation (τ < 3). Thus, these higher temperature systems may have some variability in the network structure compared to the lower temperature systems. For example, midblocks may form elastically inactive loops instead of bridges in the initial gel structure, which would ultimately decrease the maximum stress response of the sheared gel (observed here and reported elsewhere[14]). Following shear-induced fracture, if any of the loops formed bridges upon healing, this would cause a corresponding increase in the maximum stress response and result in >100% recovery.

Additional experiments were performed to determine if the strengthening effect was due to aging of the system or solvent evaporation. Prior to the primary fracture experiment, gels were held for 5−90 min at a fixed temperature (28 and 25 °C). At relatively large aging times (>30 min), significant reductions in the maximum stress were observed and attributed to syneresis-type behavior,[18−20] where recovery was significantly decreased as solvent could be expelled from the network. Aging time of <30 min displayed behavior similar to what is reported here, including >100% recovery. It is expected that solvent evaporation would cause an increase in the primary fracture stress maximum. However, at the resting times investigated here, solvent evaporation was not believed to be significant as the stress maximum of the primary fracture event of same temperatures did not vary between repeated experiments with the same gel sample.

■ ASSOCIATED CONTENT

Supporting Information

Details on the rheophysical apparatus, the gel samples, and the testing history are available, as well as complete step-strain data sets, equations, and curve fits used to determine the characteristic relaxations times that are reported in Table 1 and data related to initial gelation kinetics. This material is available free of charge via the Internet at http://pubs.acs.org.

■ AUTHOR INFORMATION

Corresponding Author

*E-mail: erk@purdue.edu.

Present Address

§Sanveo, Inc., 39899 Balentine Drive, Newark, CA 94565, U.S.A. (A.B.).

Notes

The authors declare no competing financial interest.

■ ACKNOWLEDGMENTS

We acknowledge the generous advice and guidance from Dr. Y. Thomas Hu (Halliburton Technology Center, Houston, TX) on the construction of the particle tracking flow visualization system and Prof. Steven Wereley (Purdue University) on advice related to velocimetry measurements.

■ REFERENCES

(1) Ducrot, E.; Chen, Y.; Bulters, M.; Sijbesma, R. P.; Creton, C. *Science* **2014**, *344*, 186−189.

(2) Sun, T. L.; Kurokawa, T.; Kuroda, S.; Ihsan, A. B.; Akasaki, T.; Sato, K.; Haque, M. A.; Nakajima, T.; Gong, J. P. *Nat. Mater.* **2013**, *12*, 932−937.

(3) Dowling, M. B.; Kumar, R.; Keibler, M. A.; Hess, J. R.; Bochicchio, G. V.; Raghavan, S. R. *Biomaterials* **2011**, *32*, 3351−3357.

(4) Yan, C.; Mackay, M. E.; Czymmek, K.; Nagarkar, R. P.; Schneider, J. P.; Pochan, D. J. *Langmuir* **2012**, *28*, 6076−6087.

(5) Olsen, B. D.; Kornfield, J. A.; Tirrell, D. A. *Macromolecules* **2010**, *43*, 9094−9099.
(6) Zhu, Q.; Barney, C. W.; Erk, K. A. *Mater. Struct.* **2014**, DOI: 10.1617/s11527-014-0308-5.
(7) Erk, K. A.; Henderson, K. J.; Shull, K. R. *Biomacromolecules* **2010**, *11*, 1358−1363.
(8) Erk, K. A.; Shull, K. R. *Macromolecules* **2011**, *44*, 932−939.
(9) Skrzeszewska, P. J.; Sprakel, J.; de Wolf, F. A.; Fokkink, R.; Cohen Stuart, M. A.; van der Gucht, J. *Macromolecules* **2010**, *43*, 3542−3548.
(10) Rossow, T.; Habicht, A.; Seiffert, S. *Macromolecules* **2014**, *47*, 6473−6482.
(11) Erk, K. A.; Martin, J. D.; Hu, Y. T.; Shull, K. R. *Langmuir* **2012**, *28*, 4472−4478.
(12) Gallot, T.; Perge, C.; Grenard, V.; Fardin, M.-A.; Taberlet, N.; Manneville, S. *Rev. Sci. Instrum.* **2013**, *84*, 045107.
(13) Manneville, S. *Rheol. Acta* **2008**, *47*, 301−318.
(14) Seitz, M. E.; Burghardt, W. R.; Faber, K. T.; Shull, K. R. *Macromolecules* **2007**, *40*, 1218−1226.
(15) Baumberger, T.; Caroli, C.; Martina, D. *Nat. Mater.* **2006**, *5*, 552−555.
(16) Baumberger, T.; Caroli, C.; Martina, D. *Eur. Phys. J. E* **2006**, *21*, 81−89.
(17) Billen, J. Simulated associating polymer networks. *Ph.D. Thesis*, The Claremont Graduate University, San Diego State University, San Diego, CA, 2012.
(18) Faers, M. A.; Choudhury, T. H.; Lau, B.; McAllister, K.; Luckham, P. F. *Colloids Surf. A* **2006**, *288*, 170−179.
(19) Adams, D. J.; Mullen, L. M.; Berta, M.; Chen, L.; Frith, W. J. *Soft Matter* **2010**, *6*, 1971.
(20) Liu, Y.; Lloyd, A.; Guzman, G.; Cavicchi, K. A. *Macromolecules* **2011**, *44*, 8622−8630.